

## *In situ* XPS study of Pd(1 1 1) oxidation at elevated pressure, Part 2: Palladium oxidation in the $10^{-1}$ mbar range

Harald Gabasch<sup>a</sup>, Werner Unterberger<sup>a</sup>, Konrad Hayek<sup>a</sup>, Bernhard Klötzer<sup>a</sup>,  
Evgueni Kleimenov<sup>b</sup>, Detre Teschner<sup>b</sup>, Spiros Zafeiratos<sup>b</sup>, Michael Hävecker<sup>b</sup>,  
Axel Knop-Gericke<sup>b</sup>, Robert Schlögl<sup>b</sup>, Jinyi Han<sup>c</sup>, Fabio H. Ribeiro<sup>c</sup>,  
Balazs Aszalos-Kiss<sup>d</sup>, Teresa Curtin<sup>d</sup>, Dmitry Zemlyanov<sup>d,e,\*</sup>

<sup>a</sup> Institut für Physikalische Chemie, Universität Innsbruck, A-6020 Innsbruck, Austria

<sup>b</sup> Abteilung Anorganische Chemie, Fritz-Haber-Institut der Max-Planck-Gesellschaft, Faradayweg 4-6, D-14195 Berlin, Germany

<sup>c</sup> School of Chemical Engineering, Purdue University, 480 Stadium Mall Drive, West Lafayette, IN 47907-2100, USA

<sup>d</sup> Materials and Surface Science Institute, and Physics Department, University of Limerick, Limerick, Ireland

<sup>e</sup> Birck Nanotechnology Center, Purdue University, 1205 West State Street, West Lafayette, IN 47907-2057, USA

Received 10 January 2006; accepted for publication 9 May 2006

Available online 12 June 2006

### Abstract

The oxidation of the Pd(1 1 1) surface was studied by *in situ* XPS during heating and cooling in 0.4 mbar O<sub>2</sub>. The *in situ* XPS data were complemented by *ex situ* TPD results. A number of oxygen species and oxidation states of palladium were observed *in situ* and *ex situ*. At 430 K, the Pd(1 1 1) surface was covered by a 2D oxide and by a supersaturated O<sub>ads</sub> layer. The supersaturated O<sub>ads</sub> layer transforms into the Pd<sub>5</sub>O<sub>4</sub> phase upon heating and disappears completely at approximately 470 K. Simultaneously, small clusters of PdO, PdO seeds, are formed. Above 655 K, the bulk PdO phase appears and this phase decomposes completely at 815 K. Decomposition of the bulk oxide is followed by oxygen dissolution in the near-surface region and in the bulk. The oxygen species dissolved in the bulk is more favoured at high temperatures because oxygen cannot accumulate in the near-surface region and diffusion shifts the equilibrium towards the bulk species. The saturation of the bulk “reservoir” with oxygen leads to increasing the uptake of the near-surface region species. Surprisingly, the bulk PdO phase does not form during cooling in 0.4 mbar O<sub>2</sub>, but the Pd<sub>5</sub>O<sub>4</sub> phase appears below 745 K. This is proposed to be due to a kinetic limitation of PdO formation because at high temperature the rate of PdO seed formation is compatible with the rate of decomposition.

© 2006 Elsevier B.V. All rights reserved.

**Keywords:** X-ray photoelectron spectroscopy; Chemisorption; Oxidation; Surface chemical reaction; Palladium; Single crystal surfaces; Low index single crystal surfaces; Oxygen; High-pressure XPS

### 1. Introduction

The first part of our study was dedicated to relatively low-pressure interaction of Pd(111) and oxygen in the pressure range of  $10^{-3}$  mbar [1]. This paper focuses on an

*in situ* XPS study of the palladium/oxygen interaction at 0.4 mbar O<sub>2</sub> pressure. In comparison with the literature briefly discussed in Part I [1], this publication presents one of the first data on *in situ* palladium oxidation. The *in situ* investigation allows us to propose that the key step in palladium oxidation is formation of small PdO clusters, PdO seeds. An adequate understanding of the oxidation mechanism is difficult without an *in situ* high-pressure study. From the viewpoint of thermodynamics, Warner [2] calculated an expression for the equilibrium oxygen

\* Corresponding author. Address: Birck Nanotechnology Center, Purdue University, 1205 West State Street, West Lafayette, IN 47907-2057, USA. Tel.: +1 765 496 2457; fax: +1 765 496 2457.

E-mail address: [dzemlian@purdue.edu](mailto:dzemlian@purdue.edu) (D. Zemlyanov).

pressure of the PdO/Pd couple in the range 800–1200 K. Using Warner's expression, one can work out that in 1 mbar O<sub>2</sub>, the PdO/Pd transition takes place at approximately 840 K. If this expression is extrapolated to low pressures, the PdO/Pd transition at 10<sup>-6</sup> mbar is estimated to occur at approximately 610 K. We may raise the fundamental question: *Can the catalytically active species survive reaction quenching during any kind of ex situ examination, which involves removal of the reaction gases?* Clearly, an *in situ* XPS study at elevated pressure allows researchers to overcome this problem. The surface chemical states were thus monitored *in situ* at an oxygen pressure of 0.4 mbar. At this pressure the PdO/Pd transition is calculated to occur at approximately 820 K [2], hence both palladium oxidation and oxide decomposition were investigated by heating in oxygen up to 900 K. As discussed in Part I [1], palladium oxidation at a lower pressure (2 × 10<sup>-3</sup> mbar) showed a pronounced hysteresis behaviour. Surprisingly, during cooling in oxygen a surface oxide species with hexagonal geometry and an oxygen content of ~0.4 ML appeared at a temperature 70 °C higher than the decomposition temperature of the 2D Pd<sub>5</sub>O<sub>4</sub> oxide observed during heating [1]. The hysteresis phenomenon was also studied during the heating/cooling ramps at higher oxygen pressure. The highest pressure of oxygen used in the *in situ* experiments was 0.4 mbar. This does not reflect the pressure limitation of the *in situ* high-pressure XPS spectrometer, which can operate at a few mbar pressure [3]. However, oxygen has a maximum ionization cross section at an electron kinetic energy between 100 eV and 200 eV. A pressure of 0.4 mbar is a compromise between reasonable signal intensity and the thermodynamic limit of PdO decomposition, which does not shift too much towards lower temperatures.

## 2. Experimental methods

Two experimental setups were used for this investigation. The *in situ* study was carried out in the specially designed XPS spectrometer at beamline U49/2-PGM2 at BESSY in Berlin. The sample, a (111)-oriented Pd single crystal, was mounted on a temperature-controlled heating stage. The temperature was measured by a chromel–alumel thermocouple spot-welded onto the side of the sample. The sample was heated by an IR laser from the rear. The sample cleaning procedures consisted of repeated cycles of Ar<sup>+</sup> sputtering at room- and elevated temperatures, annealing at 950 K in UHV, and exposure to O<sub>2</sub> followed by flashing at 950 K for 60 s in UHV. The sample cleanliness was checked by XPS. The typical heating/cooling rate was 10 K/min.

Surface concentrations of oxygen species were estimated by measuring the ratio between the areas of the O 1s and Pd 3p<sub>3/2</sub> peaks. The O 1s/Pd 3p<sub>3/2</sub> area ratio for the 2D oxide phase measured at the photon energy of 650 eV was used for calibration. The oxygen coverage of the 2D oxide phase was assumed to be 0.58 ML [4]. For the O

1s/Pd 3p<sub>3/2</sub> region measured with varying photon energy during the depth profiling experiments, the O 1s/Pd 3p<sub>3/2</sub> ratio was corrected for the photon-energy dependence of the atomic subshell photoionization cross sections for O 1s and for Pd 3p [5].

The TPD/STM/LEED experiments were carried out in the different UHV system, which consisted of three chambers: the UHV analysis chamber, the UHV scanning tunnelling microscope (STM) chamber and the high-pressure reaction cell. The analysis chamber housed facilities for Auger-electron spectroscopy (AES), low energy electron diffraction (LEED), and temperature programmed desorption (TPD). The STM chamber accommodated an ambient-temperature UHV STM (RHK, Inc.). The base pressure in the UHV chambers after bake out was 6 × 10<sup>-10</sup> mbar and in the high-pressure reaction cell the base pressure was below 2 × 10<sup>-8</sup> mbar. The sample could be transferred between the chambers without exposure to the ambient atmosphere.

The TPD spectra were collected by means of a RGA-200 mass-spectrometer (Stanford Research Systems) at a constant heating rate of 5 K s<sup>-1</sup>. The sample was heated by electron-bombardment from the rear. The temperature was measured by a chromel–alumel thermocouple spot-welded onto the side of the sample. The coverage was calculated by integrating the area under a TPD peak and is given in monolayers (1 monolayer = 1 ML = 1.53 × 10<sup>15</sup> atoms cm<sup>-2</sup>). Since relatively high uptakes were measured, the maximum coverage of 2.4 ML obtained by exposure to 50 L NO<sub>2</sub> at 500 K was used for calibration [6].

Pd(111) cleaning procedures consisted of repeated cycles of Ar<sup>+</sup> sputtering at room and elevated temperatures, annealing up to 1100 K in UHV, exposure to O<sub>2</sub> and NO<sub>2</sub> followed by flashing to 1100 K for 60 s in UHV. The sample cleanliness was checked by TPD, AES and LEED. NO<sub>2</sub> and O<sub>2</sub> were introduced into the analysing chamber through a capillary dozer.

Oxygen treatments for TPD/STM/LEED experiments were performed in the high-pressure reaction cell. In the reaction cell, the sample was heated by an IR lamp controlled by a Eurotherm 2408 controller. The following treatment protocol was mostly used, and any changes are specially noted. The single crystal was heated up to the desired temperature in vacuum and oxygen was introduced. After O<sub>2</sub> exposure, the sample was cooled and oxygen was pumped off simultaneously. It took less than 1 min to cool the sample to 450 K and to reach a vacuum below 10<sup>-6</sup> mbar in the reaction chamber. After this treatment, the sample was transferred into the STM and/or analysis chamber. Scanning tunnelling microscope images were obtained using Pt–Ir tips electrochemically etched in NaCl/NaNO<sub>3</sub> melt.

As has been discussed in Part I [1], the main problem in XPS analysis of the oxygen/palladium system is the overlap between the O 1s and Pd 3p<sub>3/2</sub> peaks. To resolve this matter, the O 1s/Pd 3p<sub>3/2</sub> region was directly fitted with five components: the O(I), O(II) and O(III) components for

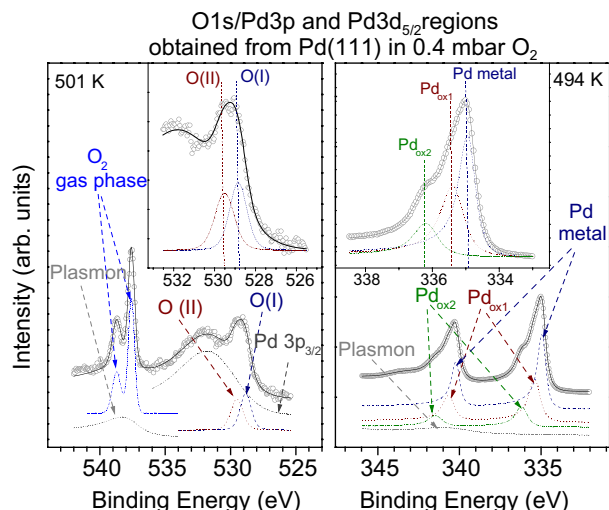


Fig. 1. Curve-fitting of the O 1s/Pd 3p Pd 3d spectra obtained from Pd(111) in 0.4 mbar O<sub>2</sub> at 500 K at photon energy 650 eV.

the O 1s signal and the Pd 3p<sub>3/2</sub> component and plasmon contribution as shown in detail in the left panel of Fig. 1. The O(III) component, which disappeared beyond 440 K, was already negligibly weak and is therefore not shown. The XPS line shape was assumed to be a Gaussian–Lorentzian function for the oxygen components and a Doniach–Sunjic function [7] for the Pd 3p<sub>3/2</sub> component and the plasmon. In the Pd 3d region both spin-orbital momentum peaks of the Pd 3d doublet were included in the curve-fitting. Therefore, the Pd 3d spectra were fitted by three pairs of Doniach–Sunjic components for Pd 3d and one pair for the plasmon excitation as shown in detail in the right panel of Fig. 1. All XPS results presented in this paper were analysed by CasaXPS software [8] and the curve-fitting procedure described above was used.

### 3. Results

#### 3.1. In situ XPS: heating in oxygen

The O 1s/Pd 3p<sub>3/2</sub> and Pd 3d spectra shown in Fig. 1 were collected from the Pd(111) surface in 0.4 mbar O<sub>2</sub>

at 501 K and 494 K. The spectra shown in Fig. 1 are typical for the 2D oxide, Pd<sub>5</sub>O<sub>4</sub> [1,4], which is characterised by two O 1s components, O(I) and O(II), at 528.92 eV and 529.52 eV and by two Pd 3d<sub>5/2</sub> components, Pd<sub>ox1</sub> and Pd<sub>ox2</sub>, at 335.50 and 336.24 eV (Table 1). The main differences to the results described in Part I [1] are that in 0.4 mbar O<sub>2</sub> the formation of the 2D oxide is completed below 500 K and the ratio between the Pd<sub>ox1</sub> and Pd<sub>ox2</sub> components is lower than the one expected for Pd<sub>5</sub>O<sub>4</sub>. These differences are discussed below.

The sets of the O 1s/Pd 3p and Pd 3d<sub>5/2</sub> core level spectra obtained at a photon energy of 650 eV *in situ* during heating the Pd(111) surface in 0.4 mbar O<sub>2</sub> are shown in Fig. 2. The O 1s/Pd 3p spectrum obtained at 438 K exhibits a broad poorly-resolved peak. The oxygen contribution consists of three components: O(I), O(II) and O(III). The O(I) and O(II) peaks are clearly features of Pd<sub>5</sub>O<sub>4</sub> (Table 1). The O(III) component centred at 530.38 eV was assigned to a supersaturated O<sub>ads</sub> layer with a coverage of 0.5 ML, corresponding to a metastable p(2 × 1) O adlayer, which has already been calculated by DFT [9]. Two oxygen-induced components, Pd<sub>ox1</sub> and Pd<sub>ox2</sub>, were distinguished in the Pd 3d<sub>5/2</sub> spectrum collected at 431 K. This fact supports formation of the 2D oxide. The spectra suggest that the Pd(111) surface was only partially covered with the 2D oxide and the other fraction of the surface was still covered with the metastable supersaturated O<sub>ads</sub> layer. This situation is quite similar to the one observed by us during low-pressure (2 × 10<sup>-3</sup> mbar) oxygen treatment [1]. In those measurements heating resulted in decreasing intensity of the O(III) component at 530.38 eV, whereas the O(I) and O(II) components started to grow. In both cases this might be interpreted as the transformation of the supersaturated O<sub>ads</sub> layer to the Pd<sub>5</sub>O<sub>4</sub> phase. In the present high-pressure experiments, the supersaturated O<sub>ads</sub> layer disappeared completely already at 469 K, at a considerably lower temperature than observed in the low-pressure experiments [1]. This fact points to a shift of the thermodynamic equilibrium situation towards the Pd<sub>5</sub>O<sub>4</sub> phase at 0.4 mbar. As the 2D Pd<sub>5</sub>O<sub>4</sub> phase was formed, the O(I)/O(II) ratio approached unity. Above 535 K, the amount of O(I) decreased slightly whereas the O(II) coverage grew

Table 1  
XPS characteristic of the oxygen species and the oxidation states discussed in Parts I and II

	Nature/conditions	Thermal stability in 0.4 mbar O <sub>2</sub>	Oxygen-induced Pd 3d <sub>5/2</sub> , eV	O 1s, eV
Supersaturated O <sub>ads</sub> layer	Adlayer with coverage of 0.5 ML	Decomposes at 470 K		530.38 ± 0.07 – O(III)
Pd <sub>5</sub> O <sub>4</sub>	Surface 2D oxide	Decomposes at approximately 800 K	335.5 ± 0.01 (Pd <sub>ox1</sub> ) 336.24 ± 0.01 (Pd <sub>ox2</sub> )	528.94 ± 0.05 – O(I) 529.55 ± 0.05 – O(II)
(√67 × √67)R12.2°	One of the phases of surface 2D oxide	–	335.44 ± 0.02 (Pd <sub>ox1</sub> )	528.94 ± 0.05 – O(I) 529.55 ± 0.05 – O(II)
PdO	Bulk oxide phase	Appears at 655 K decomposes at 815 K	336.55 (Pd <sub>ox2</sub> )	529.65 – O(II)
Dissolved oxygen	Oxygen species dissolved in the near-surface region	Desorbs at 770–870 K, diluted phase desorbs above 1070 K	N/A	528.99 ± 0.04 – O(I)

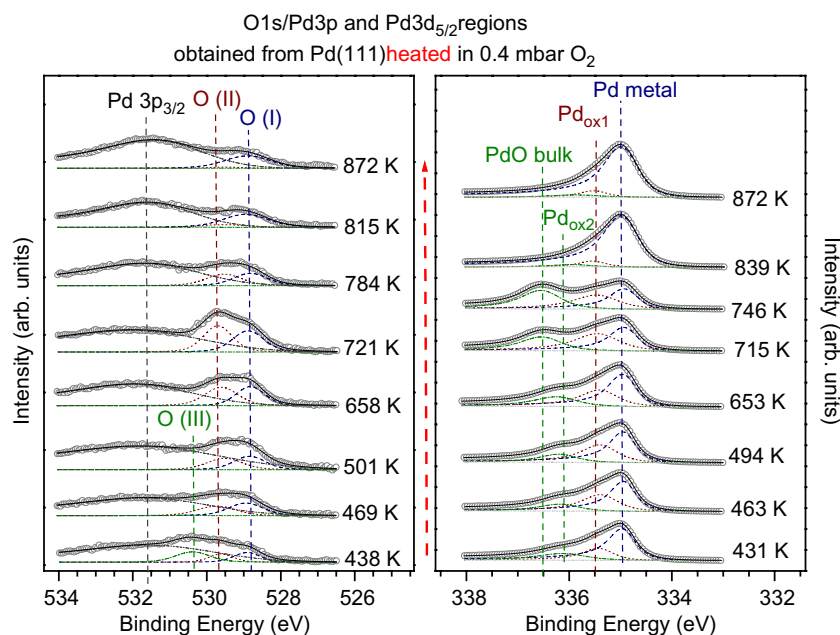


Fig. 2. The O 1s/Pd 3p Pd 3d<sub>5/2</sub> spectra collected *in situ* during heating the Pd(111) surface in 0.4 mbar O<sub>2</sub> at photon energy of 650 eV.

steadily, as shown in Fig. 4. Also the ratio between the Pd<sub>ox1</sub> and Pd<sub>ox2</sub> components is lower than 4:1 expected for Pd<sub>5</sub>O<sub>4</sub> (Fig. 4). These changes could be tentatively assigned to formation of PdO clusters, which are considered in Section 4.

Above 658 K the coverage of O(II) increased rapidly, then passed through a maximum at 753 K and sharply decreased to zero at 815 K. Simultaneously, the O(II) peak shifted towards high binding energies (BE) by 0.13–529.65 eV. The intensity and position of the O(I) component did not change much during these transformations. The Pd<sub>ox2</sub> component followed the behaviour of the O(II) peak: above 658 K the contribution of the Pd<sub>ox2</sub> component started to grow, reached the maximum at 778 K, which was followed by fast decay to zero. Also, during these transformations, the Pd<sub>ox2</sub> peak shifted towards higher BE by 0.32–336.56 eV. The changes in the temperature region from 658 K to 778 K can be interpreted in terms of the formation of the bulk oxide phase PdO (Table 1). Indeed, the position of the Pd 3d<sub>5/2</sub> peak at 336.56 eV is characteristic for bulk PdO [10–16]. The steep decrease of the O(II) coverage at the temperatures above 765 K corresponds to PdO decomposition.

The coverage of the O(I) species did not change much between 625 K and 872 K even during PdO decomposition. As discussed in Part I, in fact the O(I) peak represents two oxygen species: the lower BE oxygen species of the Pd<sub>5</sub>O<sub>4</sub> surface oxide and oxygen dissolved in the near-surface region. Above the temperature of decomposition of the 2D oxide and PdO, the O(I) peak can be assigned solely to oxygen dissolved in the near-surface region (Table 1). This species was characterised at 793 K by *in situ* XPS depth profiling and dissolution of oxygen in the palladium was confirmed [1].

The following conclusions can be drawn from the *in situ* XPS measurements during *heating* of the Pd(111) surface in 0.4 mbar O<sub>2</sub>:

1. At 431 K the surface was partially covered with the 2D oxide and a fraction of the surface was covered with a metastable supersaturated O<sub>ads</sub> layer. The Pd<sub>5</sub>O<sub>4</sub> phase is characterised by (a) the O(I) and O(II) components at 528.92 eV and 529.52 eV, respectively, with a ratio of approximately 1:1, (b) the Pd<sub>ox1</sub> and Pd<sub>ox2</sub> components at 335.5 eV and 336.24 eV, respectively, with a ratio of approximately 0.25. The O(III) component at 530.38 eV was assigned to the metastable high-coverage chemisorbed state. The surface chemical states were very similar to those observed during O<sub>2</sub> treatment at  $2 \times 10^{-3}$  mbar [1].
2. During heating the supersaturated O<sub>ads</sub> layer transforms into the 2D Pd<sub>5</sub>O<sub>4</sub> oxide phase. Small PdO clusters are supposed to form.
3. The bulk PdO phase appears above 653 K and decomposes completely at 815 K.
4. Decomposition of the bulk oxide was followed by oxygen dissolution in the bulk. Dissolved oxygen is characterised by the O 1s peak at 528.98 eV and was observed even at 873 K.

### 3.2. *In situ* XPS: cooling in oxygen

Fig. 3 shows the sets of the O 1s/Pd 3p and Pd 3d core level spectra obtained *in situ* in 0.4 mbar O<sub>2</sub> during cooling of the Pd(111) surface. The cooling experiment was started immediately after heating in 0.4 mbar O<sub>2</sub> as described in the previous section. The same rate was used for cooling

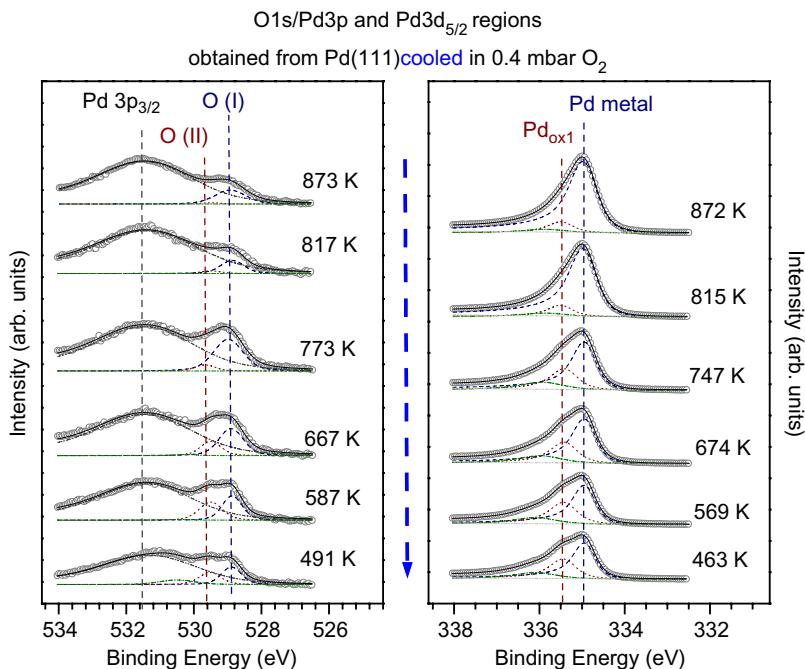


Fig. 3. The O 1s/Pd 3p Pd 3d<sub>5/2</sub> spectra collected *in situ* during cooling the Pd(111) surface in 0.4 mbar O<sub>2</sub> at photon energy of 650 eV.

and heating. The O 1s/Pd 3p spectrum collected at 873 K contained a single oxygen component, O(I), which was assigned to the near-surface region species. The contribution of the oxygen-induced Pd 3d components was almost negligible at 873 K, and the spectra suggest a metallic state of the surface with oxygen deficiency. Both the oxygen-

induced components, Pd<sub>ox1</sub> and Pd<sub>ox2</sub>, reappeared in the Pd 3d<sub>5/2</sub> spectra at 747 K. The relative ratio between the Pd<sub>ox1</sub> and Pd<sub>ox2</sub> components quickly approached the value close to the 2D Pd<sub>5</sub>O<sub>4</sub> surface oxide (Fig. 4). The oxygen-induced components were accompanied by the appearance of the O(II) component (Figs. 3 and 4). The coverage of the

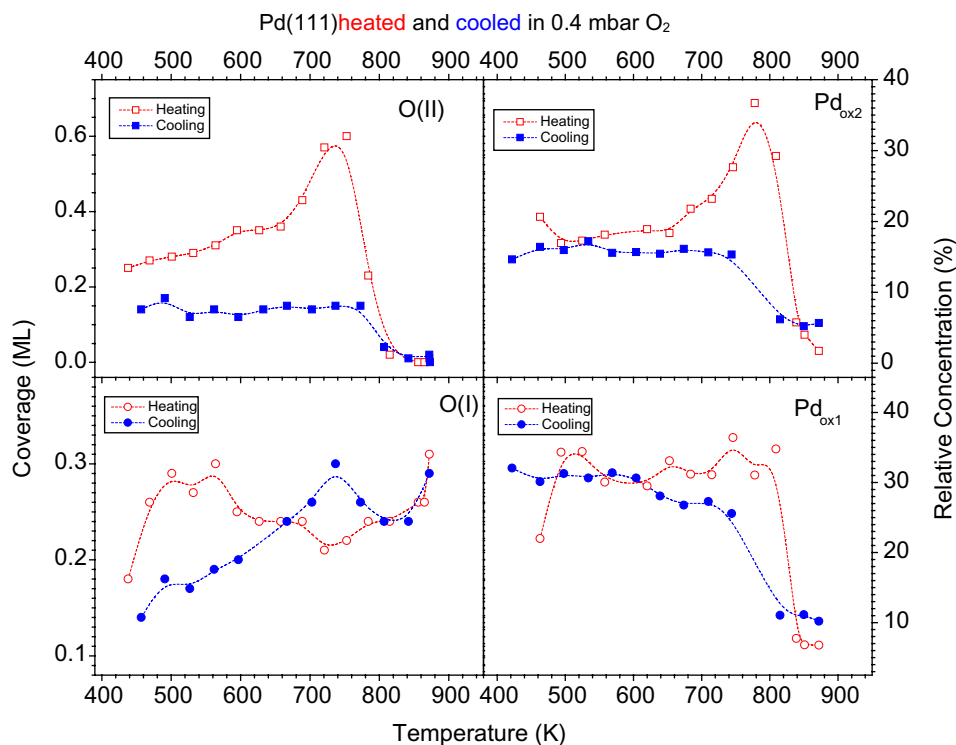


Fig. 4. Oxygen species and the oxidation states of palladium on the Pd(111) surface as a function of temperature during heating and cooling in 0.4 mbar O<sub>2</sub>. The concentration was calculated from the O 1s spectra.

O(II) species remained approximately constant during further cooling, whereas the O(I) coverage was slowly decreasing. This effect might be assigned to the decreasing contribution of oxygen dissolved in the near-surface region. The final ratio between the O(II) and O(I) components reached a value of 1.05 at 455 K. The O 1s/Pd 3p and Pd 3d core level spectra observed in this stage were characteristic for the Pd<sub>5</sub>O<sub>4</sub> phase [1]. Although this temperature was already within the PdO thermodynamic stability range, no evidence for the bulk PdO phase was observed.

The final state of the surface after cooling in 0.4 mbar O<sub>2</sub> was different from that observed after cooling in  $2 \times 10^{-3}$  mbar O<sub>2</sub> [1]. The Pd<sub>5</sub>O<sub>4</sub> 2D oxide was not observed at all during “low-pressure” cooling. Instead of the Pd<sub>5</sub>O<sub>4</sub> surface oxide, a different surface oxide phase of lower (~0.4 ML) oxygen content, probably a hexagonal ( $\sqrt{67} \times \sqrt{67}$ )R12.2° superstructure, was observed. However, during “high-pressure” cooling, the 2D oxide (O-coverage 0.58 ML) appeared. Moreover, the experiment performed in the LEED–STM–TPD experimental setup showed that a characteristic complex LEED pattern was observed on Pd(111) after exposure to 13 mbar O<sub>2</sub> for 10 min at 600 K followed by cooling in oxygen to 400 K. This LEED pattern was identical to that of the square  $\sqrt{6}$  unit cell of the Pd<sub>5</sub>O<sub>4</sub> 2D surface oxide [17]. Exposure to 1.3 mbar O<sub>2</sub> for 10 min at 820 K followed by cooling in O<sub>2</sub> to 400 K resulted in a weak (1 × 1) pattern co-existing with a diffuse LEED pattern, which was similar to the Pd<sub>5</sub>O<sub>4</sub> phase.

The conclusions which can be drawn from the *in situ* XPS measurements in 0.4 mbar O<sub>2</sub> during cooling, of the Pd(111) surface, are:

1. The bulk PdO phase does not form during cooling in 0.4 mbar O<sub>2</sub>.
2. Below 747 K the Pd<sub>5</sub>O<sub>4</sub> phase appears.

### 3.3. Temperature programmed desorption

As mentioned in the experimental section, TPD, STM and LEED experiments were carried out in the second experimental setup. The following treatment protocol was used: the single crystal was heated to the desired temperature in vacuum and oxygen was then introduced. After O<sub>2</sub> exposure, the sample was cooled and oxygen was pumped off simultaneously. Fig. 5 shows a set of oxygen TPD spectra and the corresponding oxygen uptake curve obtained after exposure of the Pd(111) single crystal to 1.3 mbar oxygen for 10 min at different temperatures between 600 K and 850 K. In order to avoid decreasing “quasi-steady-state” concentration of oxygen in the near-surface region, the single crystal was heated to 1000 K. Heating to high temperatures may lead to substantial lowering of the concentration of dissolved oxygen. In support of this statement Leisenberger et al. [18] demonstrated that in order to

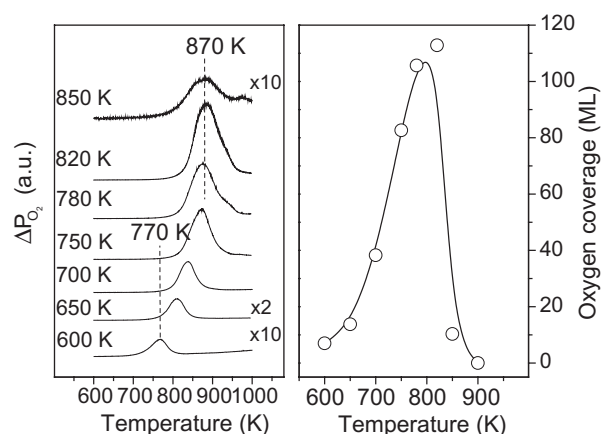


Fig. 5. TPD spectra of O<sub>2</sub> (the left panel) and oxygen uptakes on Pd(111) as a function of treatment temperature obtained from the Pd(111) single crystal exposed to 1.3 mbar of oxygen for 10 min at the specified temperatures. Oxygen uptakes on Pd(111) as a function of treatment temperature after exposure to 1.3 mbar O<sub>2</sub> for 10 min.

obtain a TPD of a 0.25 ML oxygen adlayer on the Pd(111) surface, the palladium bulk had to be saturated with oxygen, otherwise a fraction of the oxygen would irreversibly disappear in the bulk during TPD heating. In our case, the uptake was measured after repeated oxygen treatments until a constant uptake was obtained or, in other words, until the palladium bulk was saturated with oxygen.

As shown in Fig. 5, O<sub>2</sub> desorbed as a single TPD peak, which shifted from 770 K to 870 K as the temperature during dosing was increased from 600 K to 850 K. The oxygen uptake grew from an equivalent of 7 ML at 600 K to the maximum of 113 ML at 820 K. A further increase of the exposure temperature resulted in an abrupt decrease of the oxygen uptake. The most interesting fact is that no traces of oxygen were detected by AES after all the oxygen treatments, even in case of the TPD-detected desorption of the equivalent of 113 ML oxygen. On the other hand, an AES oxygen peak was observed from the Pd<sub>5</sub>O<sub>4</sub> 2D oxide. The STM measurements of tunnelling current versus bias voltage (also referred to as *I*–*V* spectroscopy) did not reveal the energy gap expected for the PdO bulk oxide. For instance, a band gap of 4.0–5.0 eV is typical for stoichiometric PdO [19,20]. This fact leads to the straightforward conclusion that the TPD spectra shown in Fig. 5 are not representative for the bulk PdO phase. According to the terminology used in the XPS section, the TPD spectra are characteristic of the oxygen species dissolved in the near-surface region. In contrast, the bulk oxide was clearly observed by *in situ* XPS as discussed above. The absence of the bulk PdO phase in the TPD experiments can be explained by the experimental procedure. Likely, the bulk PdO phase and other surface-related oxide phases, for instance, the Pd<sub>5</sub>O<sub>4</sub> phase, decomposed during quenching after the oxygen treatment. Also, TPD protocol corresponds to the cooling ramp in the *in situ* XPS experiments when PdO was not observed. According to *in situ* XPS, the

amount of the oxygen species in the near-surface region is estimated to be approximately 0.25 ML. Assuming an information depth for photoelectrons with 120 eV kinetic energy of 12 Å [21] and a lattice parameter for Pd(111) of 2.25 Å, the average oxygen concentration in one single Pd layer is calculated to be approximately 0.05 ML. Keeping the equivalent of 113 ML measured by TPD in mind, one can safely deduct that oxygen diffuses to a significant depth. Oxygen dissolution in the palladium bulk resulted in metal lattice expansion. Thus, after 1.3 mbar O<sub>2</sub> at 600 K, the step height was  $2.45 \pm 0.1$  Å, whereas the step height on the clean Pd(111) surface was  $2.25 \pm 0.05$  Å.

As mentioned in the XPS section above, the change of the treatment protocol revealed another phenomenon. Usually the sample was cooled and oxygen was pumped off *simultaneously*. The complex LEED pattern of the 2D surface oxide [17] was observed after 1.3 mbar O<sub>2</sub> treatment for 10 min at 600–820 K when the sample was cooled to 400 K in oxygen. The quality of the LEED pattern depended on the treatment temperature. The observation of the 2D oxide by LEED is in agreement with our *in situ* XPS results. Diffusion of oxygen into the palladium bulk should be hindered at low temperature and, therefore, a rather high concentration of oxygen could accumulate in the near-surface region and this could create a favourable situation for 2D surface oxide growth. Also, a high concentration of the near-surface oxygen species may help to stabilize Pd<sub>5</sub>O<sub>4</sub>.

A comparison between *in situ* XPS and TPD experiments allowed us to make another interesting observation. Fig. 6 shows O<sub>2</sub> TPD traces obtained after exposure of the Pd(111) surface to 1.3 mbar O<sub>2</sub> at 820 K, 850 K and 900 K. The TPD heating was extended up to 1300 K. The experimental history was the same for all experiments: the sample was sputtered by Ar<sup>+</sup> and annealed in UHV. As seen in Fig. 5, besides the main TPD peak at 865 K, a high-temperature peak at 1130 K appeared. The high-temperature peak cannot be due to an artefact. In order to rule out desorption from the sample holder, the Pd(111) single crystal was replaced for a stainless steel disk and no oxygen desorption was observed after identical treatments. The high-temperature TPD feature was reported in the literature [18,22,23] and was assigned to dissolved oxygen. The amount of highly stable oxygen increased with the treatment temperature. Thus the equivalent of 2 ML and 8 ML were measured after O<sub>2</sub> exposure at 820 K and 900 K, respectively.

The conclusions from the *ex situ* TPD/STM study in 1.3 mbar O<sub>2</sub> are:

1. The TPD results were consistent with the *in situ* XPS findings. TPD demonstrated massive dissolution of oxygen in the palladium bulk. The oxygen uptake was equivalent to 113 ML, measured after 1 mbar O<sub>2</sub> treatment at 820 K for 10 min.
2. Oxygen dissolution might cause changes of the lattice parameters.

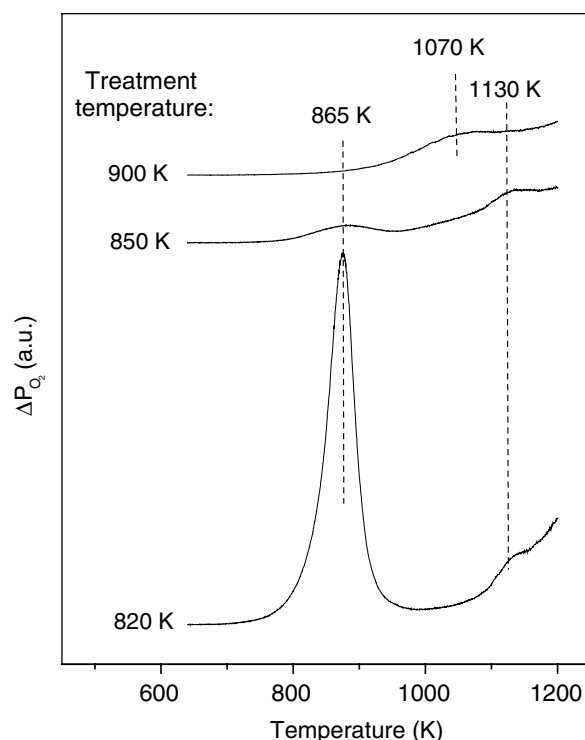


Fig. 6. TPD spectra of O<sub>2</sub> obtained after exposure the Pd(111) single crystal to 1.3 mbar oxygen for 10 min at 820 K, 850 K and 900 K. TPD was carried out up to 1300 K.

3. Another stable oxygen species was detected by TPD. This oxygen species desorbs at temperatures above 1050 K. The relationship between different oxygen species is discussed below.

#### 4. Discussion

The results of the *in situ* XPS study of the Pd(111)-oxygen interaction at  $2 \times 10^{-3}$  mbar O<sub>2</sub> were discussed in Part I [1]. Part II focuses on the *in situ* XPS investigation at a higher oxygen pressure of 0.4 mbar; the results are complemented by *ex situ* TPD data. The main difference between low-pressure ( $2 \times 10^{-3}$  mbar) and high-pressure (0.4 mbar) experiments is (1) that the formation of the bulk PdO phase was detected only at 0.4 mbar, and (2) that during cooling the formation of the Pd<sub>5</sub>O<sub>4</sub> surface oxide was only observed at 0.4 mbar. It is interesting that, according to Warner's expression for the equilibrium oxygen pressure of the PdO/Pd system [2], PdO should be the stable phase up to 740 K in  $2 \times 10^{-3}$  mbar O<sub>2</sub> and up to 820 K in 0.4 mbar O<sub>2</sub>. However, in  $2 \times 10^{-3}$  mbar O<sub>2</sub> the bulk PdO phase did not form either during heating or cooling. At 0.4 mbar O<sub>2</sub> PdO was detected only during heating. It seems now clear that the palladium/oxygen system cannot be described just by the simple thermodynamic transition Pd ↔ PdO. Other processes, such as the diffusion of oxygen to the palladium bulk, and the formation of different 2D oxide phases, must be considered. The experimental

facts represented above allow us to propose that palladium oxidation is kinetically limited.

As discussed in Section 3, at 535 K the ratio between the  $\text{Pd}_{\text{ox1}}$  and  $\text{Pd}_{\text{ox2}}$  components is lower than 4:1 expected for  $\text{Pd}_5\text{O}_4$  (Fig. 4). Increasing of the  $\text{Pd}_{\text{ox2}}$  component could be assigned to formation of PdO clusters, which serve as “seeds” for bulk PdO. This hypothesis is consistent with all experimental results. Also it is remarkable that the characteristic features of the 2D oxide were observed during PdO growth (Fig. 4). This may be explained by three-dimensional island growth of bulk PdO starting at defects of the mainly  $\text{Pd}_5\text{O}_4$ -covered surface. For instance, Gabasch et al. [9] demonstrated that oxidation preferentially starts at the steps.

In order to better understand the oxidation mechanism, the experimental data represented in Fig. 4 were re-plotted as show in Figs. 7 and 8 with the following assumptions made. Since during heating between 470 K and 595 K the ratio between the O(I) and O(II) components was approximately at 1:1, the excess of the O(II) component was assigned to bulk PdO. Above 800 K, neither PdO nor 2D oxide can be present on the surface and the O(I) peak can be assigned exclusively to the oxygen species dissolved in the near-surface region. For the heating ramp, three temperature regions can be distinguished (Figs. 7 and 8). The first region, which ranges from 440 K to 565 K, corresponds to the formation of the 2D oxide phase and PdO “seeds”. The O 1s and Pd 3d components, which are characteristic of the surface oxide, remain approximately constant during this stage. Monatomic-deep hexagonal holes were observed by *ex situ* STM [24] after 1.3 mbar treatment in  $\text{O}_2$  at 600 K. These holes are typical for post-reaction of the  $\text{Pd}_5\text{O}_4$  phase with the residual gases or partial desorption of  $\text{Pd}_5\text{O}_4$  during pump-off [4]. The conclusion is that

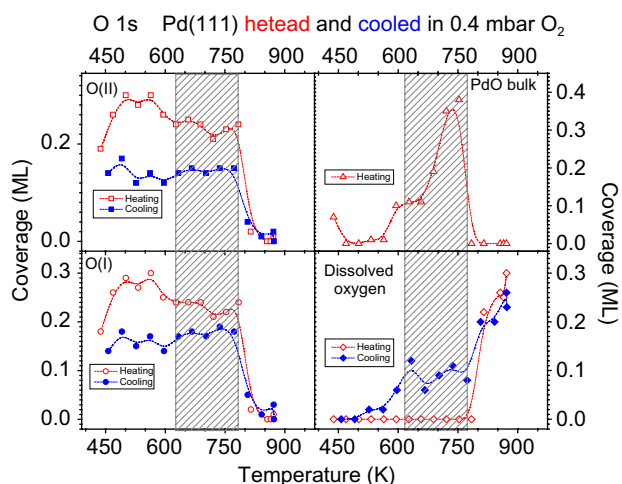


Fig. 7. Oxygen species and the oxidation states of palladium on the Pd(111) surface as a function of temperature during heating and cooling in 0.4 mbar  $\text{O}_2$ . The concentrations shown in Fig. 4 were corrected as described in the text.

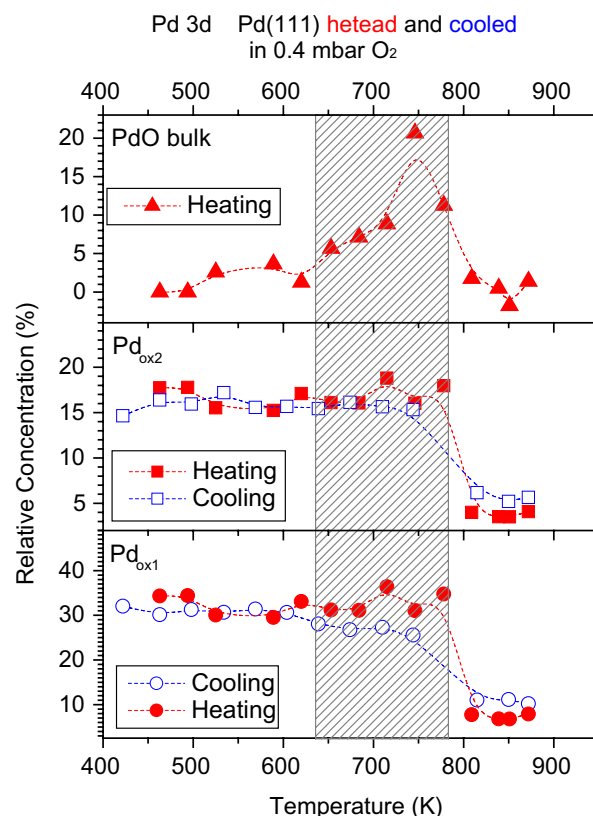


Fig. 8. The oxidation states of palladium on the Pd(111) surface as a function of temperature during heating and cooling in 0.4 mbar  $\text{O}_2$ . The concentrations shown here were obtained by correction of the data shown in Fig. 4 as described in the text.

in the temperature window between 440 K and 565 K the 2D oxide phase forms from the supersaturated  $\text{O}_{\text{ads}}$  layer.

The second temperature region is from 565 K to 780 K, when the coverage of the 2D oxide decreases and the PdO phase starts to grow. The slow growth at temperatures below 675 K is followed by an acceleration of the formation rate and the PdO concentration reaches a maximum at approximately 750 K (Figs. 7 and 8). This observation strongly suggests that although PdO is the thermodynamically most stable phase at low temperatures [9], the PdO growth is essentially kinetically limited. One of the facts supporting this observation is that no bulk PdO phase formed during the cooling ramp in 0.4 mbar  $\text{O}_2$ . Bulk PdO formation requires the PdO seeds, whereas at high temperature the equilibrium is shifted towards dissolution of oxygen in the palladium bulk and the overall rate of the PdO seed formation is low. At lower temperature, when the 2D oxide started to form, the concentration of dissolved oxygen decreases. The 2D oxide likely inhibits oxygen dissolution. As it was demonstrated in Ref. [24], oxygen dissolution in the palladium bulk is limited by diffusion through an oxide layer. So in our case, the  $\text{Pd}_5\text{O}_4$  phase might play the role of a “preserving” layer. Also during the cooling ramp, a phase of the 2D oxide, which is not favourable for PdO seeds, might form.

The third temperature region is above 780 K and it is characterised by PdO decomposition and oxygen dissolution in the palladium bulk. The upper thermal stability limit of PdO is close to the expected thermodynamic limit. The rate of oxygen dissolution likely depends on the oxygen pressure. Thus at  $2 \times 10^{-3}$  mbar the quasi-steady oxygen concentration in the near-surface region was an equivalent of approximately 0.15 ML (Part I [1], Fig. 9) whereas at 0.4 mbar (Fig. 7) the corresponding figure was an equivalent of 0.25 ML. This difference likely reflects divergence of the oxygen concentration on the surface at low and high pressures because diffusion into the bulk is limited by the temperature only. According to STM data, accommodation of the oxygen species in the palladium lattice resulted in increasing height of monatomic steps and this might be explained by the metal lattice expansion. Oxygen diffusion in the palladium bulk is an activated process with apparent activation energy of  $84 \text{ kJ mol}^{-1}$  [24].

The TPD experiment clearly showed two oxygen species desorbed at 870 K and above 1070 K. The high-temperature desorption peak can be attributed to dilute solid solution of oxygen in the palladium bulk, but in the near-surface region a high concentration of oxygen may locally achieve a critical value required for phase transformation and this would result in the TPD peak at 870 K. Likely, dilute oxygen does not affect considerably the surface properties. On the other hand, oxygen dissolved in the palladium bulk is essential to facilitate the formation of the “ordered” oxygen in the near-surface region. Thus, as discussed in Section 3, the concentration of near-surface oxygen increases as the bulk species accumulates and the concentration of near-surface oxygen decreases when the oxygen population in the bulk is depleted by heating to 1300 K. Indeed, since oxygen diffusion in the bulk is proportional to the concentration gradient, at low concentration of oxygen dissolved in the bulk the equilibrium should be shifted towards oxygen diffusing in the bulk and it would be difficult to achieve a high concentration of oxygen in the near-surface region. As soon as the bulk “reservoir” is filled with oxygen, diffusion in the bulk slows down and the uptake of the near-surface oxygen increases. A similar effect was described in the literature by Leisenberger et al. [18], who observed the transformation of the chemisorbed oxygen to the dissolved species. These researchers also pointed to that in order to yield quantitatively reproducible oxygen desorption from the  $p(2 \times 2)$  structure, the palladium bulk must be filled with oxygen.

It is interesting that the oxygen behaviour discussed above appears to be similar for both hydrogen and carbon species in Pd. Thus, for instance small amounts of interstitial hydrogen form a disordered solid solution in palladium. If the concentration of the disordered hydrogen increases, the structured Pd hydride phase appears. For carbon, the well known interstitial solid solution  $\text{PdC}_x$  with  $x$  up to  $\sim 0.15$  exists. A new structured phase of carbon with a much larger  $x$  was observed during ethene oxidation on Pd(111) [25]. This state can only be approached *in situ*.

## 5. Summary

*In situ* XPS was used to study the oxidation of single crystal Pd(111) during heating and cooling in 0.4 mbar  $\text{O}_2$ . *In situ* XPS results were complemented with *ex situ* TPD data. This paper along with Part I [1] demonstrated that it is possible to follow the mechanism of palladium oxidation by *in situ* XPS. The comparison of *in situ* XPS and TPD data highlights the advantage of the *in situ* technique, which is the possibility to monitor the oxygen/palladium interaction without quenching the reaction.

A number of oxygen species and oxidation states of palladium were observed (Table 1). The 2D oxide,  $\text{Pd}_5\text{O}_4$ , was characterised by two O 1s components at 528.92 eV and 529.52 eV and by two oxygen-induced Pd  $3d_{5/2}$  components at 335.5 eV and 336.24 eV. The supersaturated  $\text{O}_{\text{ads}}$  layer exhibits the O 1s core level peak at 530.37 eV. Oxygen dissolved in the near-surface region was identified by the O 1s core level peak at 528.98 eV and by a TPD peak at 770–870 K. The dilute solid solution of oxygen in the palladium bulk was found to desorb at temperatures above 1070 K.

The following scenario of the interaction between palladium and oxygen at 0.4 mbar is proposed:

1. At 430 K, similarly to the  $3 \times 10^{-3}$  mbar  $\text{O}_2$  case, the Pd(111) surface is partially covered by the 2D oxide phase and the other fraction of the surface is covered by the supersaturated  $\text{O}_{\text{ads}}$  layer. During heating the supersaturated  $\text{O}_{\text{ads}}$  layer transformed into the  $\text{Pd}_5\text{O}_4$  phase. However, the supersaturated  $\text{O}_{\text{ads}}$  layer disappears completely at approximately 470 K, a temperature considerably lower than observed in the low-pressure experiments [1].
2. Above 655 K, the bulk PdO phase appears and this phase decomposes completely at approximately 815 K. It is proposed that small PdO clusters formed on the 2D oxide phase acts as a precursor for bulk PdO.
3. Decomposition of the bulk oxide is followed by oxygen dissolution in the near-surface region. The formation of the dissolved oxygen species results in expansion of the metal lattice.
4. Remarkably, the bulk PdO phase does not form during cooling in 0.4 mbar  $\text{O}_2$  but the  $\text{Pd}_5\text{O}_4$  phase appears below 750 K. The formation of the  $\text{Pd}_5\text{O}_4$  phase is completed at a temperature too low for further bulk PdO transformation.

## Acknowledgements

This work was supported by the European Community – Research Infrastructure Action under the FP6 “Structuring the European Research Area” Programme (through the Integrated Infrastructure Initiative” Integrating Activity on Synchrotron and Free Electron Laser Science – Contract R II 3-CT-2004-506008). It was also supported by Enterprise Ireland through International collaboration

Programme (IC/2004/099). D.Z. received a research scholarship from the Foundation of the University of Limerick. H.G. acknowledges a grant from the Max Planck Society. We gratefully acknowledge BESSY staff for the support during the beamtime. F.H.R. gratefully acknowledges support from the Office of Basic Energy Sciences, Chemical Sciences, US Department of Energy, grant DE-FG02-03ER15408.

## References

- [1] D. Zemlyanov, B. Aszalos-Kiss, E. Kleimenov, D. Teschner, S. Zafeiratos, M. Havecker, A. Knop-Gericke, R. Schlögl, H. Gabasch, W. Unterberger, K. Hayek, B. Klötzer, *Surf. Sci.* 600 (2006) 983.
- [2] J.S. Warner, *J. Electrochem. Soc.* 114 (1967) 68.
- [3] H. Bluhm, M. Havecker, A. Knop-Gericke, E. Kleimenov, R. Schlögl, D. Teschner, V.I. Bukhtiyarov, D.F. Ogletree, M. Salmeron, *J. Phys. Chem. B* 108 (2004) 14340.
- [4] E. Lundgren, G. Kresse, C. Klein, M. Borg, J.N. Andersen, M. De Santis, Y. Gauthier, C. Konvicka, M. Schmid, P. Varga, *Phys. Rev. Lett.* 88 (2002) 246103/1.
- [5] J.J. Yeh, I. Lindau, *At. Data Nucl. Data Tables* 32 (1985) 1.
- [6] G. Zheng, E.I. Altman, *Surf. Sci.* 462 (2000) 151.
- [7] S. Doniach, M. Sunjic, *J. Phys. C* 31 (1970) 285.
- [8] N. Fairley, CasaXPS, Neal Fairley, 1999–2006.
- [9] H. Gabasch, W. Unterberger, K. Hayek, B. Klötzer, C. Klein, M. Schmid, P. Varga, G. Kresse, *Surf. Sci.* 600 (2006) 2005.
- [10] K.S. Kim, A.F. Gossman, N. Winograd, *Anal. Chem.* 46 (1974) 197.
- [11] L.P. Haack, K. Otto, *Catal. Lett.* 34 (1995) 31.
- [12] M. Peuckert, *J. Phys. Chem.* 89 (1985) 2481.
- [13] A. Tressaud, S. Khairoun, H. Tohara, N. Watanabe, *Z. Anorg. Allg. Chem.* 540–541 (1986) 291.
- [14] J.M. Tura, P. Regull, L. Victori, M. Dolors de Castella, *Surf. Interface Anal.* 11 (1988) 447.
- [15] J.Z. Shyu, K. Otto, W.L.H. Watkins, G.W. Graham, R.K. Belitz, H.S. Gandhi, *J. Catal.* 114 (1988) 23.
- [16] R.S. Monteiro, D. Zemlyanov, J.M. Storey, F.H. Ribeiro, *J. Catal.* 199 (2001) 291.
- [17] E.H. Voogt, A.J.M. Mens, O.L.J. Gijzeman, J.W. Geus, *Surf. Sci.* 373 (1997) 210.
- [18] F.P. Leisenberger, G. Koller, M. Sock, S. Surnev, M.G. Ramsey, F.P. Netzer, B. Klötzer, K. Hayek, *Surf. Sci.* 445 (2000) 380.
- [19] C.Q. Sun, *Surf. Rev. Lett.* 7 (2000) 347.
- [20] J. Han, G. Zhu, D.Y. Zemlyanov, F.H. Ribeiro, *J. Catal.* 225 (2004) 7.
- [21] S. Tanuma, C.J. Powell, D.R. Penn, *Surf. Interface Anal.* 21 (1993) 165.
- [22] H. Conrad, G. Ertl, J. Kueppers, E.E. Latta, *Surf. Sci.* 65 (1977) 235.
- [23] D.L. Weissman, M.L. Shek, W.E. Spicer, *Surf. Sci.* 92 (1980) L59.
- [24] J. Han, D. Zemlyanov, F.H. Ribeiro, *Surf. Sci.*, in press, doi:10.1016/j.susc.2006.04.042.
- [25] H. Gabasch, W. Unterberger, K. Hayek, B. Klötzer, E. Kleimenov, D. Teschner, S. Zafeiratos, M. Havecker, A. Knop-Gericke, R. Schlögl, B. Aszalos-Kiss, D. Zemlyanov, *J. Catal.*, submitted for publication.